# IL-2Rα KO mice exhibit maternal microchimerism and reveal nuclear localization of IL-2Rα in lymphoid and non-lymphoid cells

Victoria A. Wong[1], Kristie N. Dinh[2], Guangchun Chen[3], and Lucile E. Wrenshall[1,4*]

1 Department of Neuroscience, Cell Biology, and Physiology, Boonshoft School of Medicine, Wright State University, Dayton OH 45435

2 Department of Biological Sciences, Wright State University, Dayton, OH 45435.
Current address: SpringCreek Fertility, Dayton, OH 45459

3 Genomics and Microarray Core Facility, University of Texas Southwestern Medical Center Dallas, TX 75235

4 Department of Medical Education, Boonshoft School of Medicine, Wright State University, Dayton OH 45435

***Correspondence:**
Corresponding author
lucile.wrenshall@wright.edu

Running title: IL-2Rα knock out mice express IL-2Rα
word count = 4640

keywords: IL-2Rα, knock out, maternal microchimerism, nucleus, proliferation

**Abstract**

IL-2Rα KO mice have been instrumental to discovering the immunoregulatory properties of IL-2Rα. While initially thought of only as a stimulatory cytokine, IL-2 and IL-2Rα knock out (KO) mice revealed that this cytokine-receptor system controls immune responses through restimulation-induced cell death and by promoting the survival of T regulatory cells. Although described mostly in the context of lymphocytes, recent studies by our laboratory showed that IL-2R is expressed in smooth muscle cells. Given this finding, we sought to use IL-2Rα knock mice to determine the function of this receptor in vascular smooth muscle cells. Surprisingly, we found that IL-2Rα knock out vascular smooth muscle cells had detectable IL-2Rα. Further studies suggested that the source of IL-2Rα protein was likely maternal heterozygous cells present in KO offspring due to maternal microchimerism. Because the KO was generated by using a neomycin resistance gene insert, we treated cells with G418 and were able to eliminate the majority of IL-2Rα expressing cells. This elimination revealed that IL-2Rα KO vascular smooth muscle cells exhibited increased proliferation, decreased size, and hypodiploid DNA content when compared to wildtype cells. Our findings suggest that the phenotype of complete IL-2Rα loss is more severe than demonstrated by IL-2Rα KO mice, and that IL-2Rα plays a here-to-fore unrecognized role in regulating cell proliferation in non-lymphoid cells.

## Introduction

IL-2Rα, or CD25, is a key subunit of the tripartite IL-2 receptor. Expression of IL-2Rα distinguishes activated from naïve T cells, and high expression serves as a marker for T regulatory cells. The contribution of IL-2Rα to T regulatory cell survival and prevention of autoimmunity has been demonstrated through IL-2Rα knock out (KO) mice, which develop splenomegaly, lymphadenopathy, anemia, and inflammatory bowel disease (1,2). IL-2Rα KO mice have been instrumental in determining the impact of IL-2Rα on the immune system (1,3–5).

Although the IL-2R is best known for its expression on lymphocytes, there are limited reports demonstrating the expression of IL-2R on other cell types, particularly dendritic cells (6–8). Our laboratory recently reported that vascular smooth muscle cells (VSMC) express all 3 subunits of the IL-2R (9). We found that expression of the IL-2Rα differed with VSMC phenotype, with proliferating VSMC expressing lower levels of IL-2Rα than differentiated VSMC.

To help define the function of IL-2Rα in VSMC, we sought to study cell properties in the absence of IL-2Rα. To this end, we isolated VSMC from IL-2Rα wildtype (WT) and KO mice. Surprisingly, we found that IL-2Rα protein was present, mainly in the nucleus, of both WT and KO VSMC. IL-2Rα was detected in IL-2Rα KO VSMC and splenocytes by immunofluorescence, flow cytometry, and Western blot analysis. Low levels of WT *IL2RA* were detected in genomic DNA extracted from multiple IL-2Rα KO tissues. Our studies suggest that the source of *IL2RA* DNA, and in turn IL-2Rα protein, is maternal microchimerism. The magnitude and pervasive nature of the IL-2Rα protein in KO mice is likely due to our finding that IL-2Rα protein has a surprisingly long half-life, and that IL-2Rα protein can be transferred between cells.

## Materials and Methods

*Materials and animals*

Animal studies were approved by the Institutional Animal Care and Use Committee at Wright State University and conformed to the Guide for the Care and Use of Laboratory Animals (NIH Publication, 8th edition). Heterozygous breeding pairs of IL-2Rα null (B6;129S4-*IL-2ra*$^{tm1Dw}$/J) mice were purchased from The Jackson Laboratory (Bar Harbor, ME, USA) for the establishment of breeding colonies (1).

Antibodies recognizing IL-2Rα were from the following sources: rabbit anti-human polyclonal anti-IL-2Rα antibodies were from Bioss Antibodies, Inc. (Woburn, MA), BosterBio (Pleasanton, CA), and LSBio (Seattle, WA). Mouse anti-human and anti-mouse IL-2Rα, clone 1B5D12, was from Genetex (Irvine, CA). Rabbit anti-phospho-CD25 (ser268) was from Sigma (St. Louis, MO). Rat anti-mouse CD16/32, rat anti-mouse CD4, and rat anti-mouse IL-2Rα (clone PC61) were from Biolegend (San Diego, CA). Purified mouse IL-2Rα was from SinoBiological (Wayne, PA). Antibodies used for SMC identification were as follows: rabbit anti-human smooth muscle cell alpha actin was from Novus (Littleton, CO). Sheep anti-transgelin (multiple species) was from R&D Systems (Minneapolis, MN). Rabbit anti-human h-caldesmon was from Proteintech (Rosemont, IL). Benzonase® was from Minnebio (St. Paul, MN). DMEM was from ThermoFisher (Waltham, MA).

*VSMC culture*

Murine VSMC were isolated from thoraco-abdominal aortas by enzymatic digestion based on a protocol from Kwartler, et al (10). Aortas were dissected free of adipose tissue *in situ*, removed and rinsed three times in sterile Hanks' balanced salt solution, then digested at 37°C for 16-18h with a mixture of 0.1 mg/ml collagenase (Sigma), 25 μg/ml trypsin inhibitor (Sigma) and 18 μg/ml elastase (Worthington Biochemical Corp., Lakewood, NJ). Isolated smooth muscle cells and any remaining tissues were then washed and cultured in DMEM with 10% FBS at 37°C and 5% $CO_2$. Tissue debris

66 was removed the following day.
67 For serum free conditions, VSMC were cultured in DMEM supplemented with insulin,
68 transferrin, and selenium (ITS; Sigma) (11). Identification of cells as VSMC was confirmed through
69 expression of smoothelin (passage 1-2 only), smooth muscle cell α-actin, transgelin, and h-caldesmon.
70 Human VSMC were isolated from pieces of aorta using the explant technique (9). Tissues were
71 washed with PBS and all adipose was removed. The artery was then cut into small (approximately 5
72 mm x 5 mm) pieces and 2-3 pieces per well were placed lumen side down into 6 well tissue culture
73 plates. Pieces were allowed to adhere briefly, then smooth muscle cell media (ScienCell, Carlsbad,
74 CA) supplemented with 10% FBS was carefully added to the wells so as not to dislodge the pieces of
75 aorta. The tissue was maintained at 37°C and SMCs were harvested in 3 - 4 weeks. VSMC were then
76 passaged every 7 - 8 days and used after 1-2 passages.
77
78 *PCR and qPCR*
79 Offspring of heterozygous breeding pairs of IL-2Rα null (B6;129S4-*IL-2ra*$^{tm1Dw}$/J) mice were
80 genotyped per Jax mice touchdown protocol (12). Briefly, DNA was extracted from tail clippings and
81 amplified using the recommended primers and touchdown protocol. Primers were as follows: (WT
82 forward CTGTGTCTGTATGACCCACC, WT reverse CAGGAGTTTCCTAAGCAACG; mutant
83 forward CTTGGGTGGAGAGGCTATTC, mutant reverse AGGTGAGATGACAGGAGATC). The
84 WT primer sequences are contained within exon 2.
85 Quantitative real time PCR was performed, using the above primers, with 15 ng genomic DNA
86 input in triplicate on a 7500 fast real-time PCR system (Applied Biosystems, ThermoFisher Scientific)
87 using PowerUp™ SYBR™ Green Master Mix kit (Applied Biosystems) according to the
88 manufacturer's instructions. The cycle profile was 2 minutes at 50 °C, 2 minutes at 95 °C, 40 cycles of
89 3 seconds at 95 °C and 30 seconds at 60 °C. GAPDH was used as an endogenous control. RT-minus
90 and no template controls (NTC) were included for negative control. Data were analyzed using 7500
91 software v2.3 (Applied Biosystems).
92
93 *Flow cytometry*
94 Splenocyte cell suspensions were prepared by mechanical disruption of the spleen followed by
95 filtration to remove large pieces of noncellular debris. The following incubations were all performed
96 on ice. Splenocytes were first incubated with anti-CD16 (TruStain, FcX) for 15 min, then washed and
97 stained with the indicated anti-IL-2Rα antibodies for 30 minutes. Following fixation in 2%
98 paraformaldehyde, intracellular staining was performed by first permeabilizing cells via suspension in
99 ice cold methanol for 30 minutes. Cells were then washed twice in PBS with 2% BSA and stained with
100 anti-IL-2Rα antibodies for 30 minutes. Clone PC 61.5 and anti-IL-2Rα from Genetex were directly
101 conjugated to Cy-5 fluorochromes and anti-IL-2Rα from Boster was used with a Cy5 labeled
102 secondary antibody. A subset of cells was treated with Benzonase® 250U/$10^6$ cells for 50 minutes at
103 37°C prior to staining. Data were acquired on a Accuri C6 flow cytometer (Bectin Dickinson, Franklin
104 Lakes, NJ) and analyzed using FCS Express 7 (Pasadena, CA).
105
106 *Microscopy*
107 VSMC were cultured in chamber slides and fixed in ice cold methanol with 2% acetic acid.
108 Fixed VSMC were then washed with PBS and blocked for 1h using Odyssey blocking solution (LI-
109 COR, Lincoln, NE). Blocking solution was removed by washing, and primary antibodies were diluted
110 in TBST (10 mM Tris, pH 8.0, 150 mM NaCl, 0.5% Tween 20) and applied to cells overnight at 4°C.
111 The primary antibody was removed by washing, and the appropriate fluor-conjugated secondary was
112 applied for 1h. Cells were imaged on an EVOS epifluorescent microscope (ThermoFisher) or on a

113 Cytation imaging plate reader (Biotek, Winooski, VT). Images from the Cytation were processed using
114 the flow cytometry software FCS Express 7.
115
116 *Western blot analysis*
117 Whole cell lysates from primary VSMCs and Jurkat T cells (ATCC, Manassas, VA) were
118 prepared by lysing and sonicating pelleted cells in radio immuno-precipitation (RIPA) buffer (150 mM
119 NaCl, 25 mM Tris-HCl pH 7.6, 1% Nonidet P40, 1.0 % sodium deoxycholate, 0.1 % SDS).
120 Splenocytes were separated into membrane, cytoplasmic, and nuclear fractions per manufacturer's
121 instructions (Cell Fractionation Kit, Cell Signaling Technology, Danvers, MA). Extracts were then
122 separated by SDS-PAGE, using 30 μg protein measured by bicinchoninic acid assay (Pierce, Thermo-
123 Fisher), and transferred to a polyvinylidene difluoride membrane. Some blots, as indicated in figure
124 legends, were assessed for total protein using either stain-free gels (Bio-Rad, Hercules, CA) or the
125 Revert™ 700 Total Protein Stain (LI-COR) prior to blocking. After incubation with 5% nonfat milk in
126 TBST for 60 min, the membrane was incubated with antibodies against IL-2Rα at 4 °C for 18 h.
127 Membranes were washed three times for 10 min and incubated with a 1:10,000 dilution of horseradish
128 peroxidase-conjugated anti-rabbit antibodies (Jackson ImmunoResearch, West Grove, PA) at room
129 temperature for 2 hrs. Blots were washed with TBST three times and developed with the ECL system
130 (Luminata Crescendo, Millipore Sigma) according to the manufacturer's instructions.
131
132 *Protein half-life*
133 The half-life of IL-2Rα was measured using a protocol designed by Morey, et al (13) in which
134 a traditional pulse-chase experiment was performed using L-azidohomoalanine (AHA), a methionine
135 analog, as the pulsed label. Incorporation of AHA into nascent proteins was detected by a click
136 chemistry based, copper-free strain-promoted alkyne-azide cycloaddition reaction in which a
137 fluorescent cyclooctyne probe (dibenzocyclooctyne-488) bound to incorporated AHA (14,15).
138 Specifically, VSMC were washed then cultured in methionine free DMEM with 5% dialyzed
139 FBS containing 50 μM L-azidohomoalanine (AHA) for 48 hours (duration determined by pilot
140 experiments) then cells were returned to DMEM with 10% FBS. VSMC were pelleted at indicated
141 time intervals following this initial pulse and then processed together. Because IL-2Rα is primarily
142 localized to the nucleus in VSMC, we focused on extracting nuclear proteins. Nuclear fractions were
143 isolated following the protocol outlined by Senichkin, et al (16). Briefly, pelleted cells were incubated
144 in a hypotonic buffer (20 mM Tris-HCl (pH 7.4), 10 mM KCl, 2 mM $MgCl_2$, 1 mM EGTA, 0.5 mM
145 DTT, 0.5 mM PMSF) for 3 minutes, followed by addition of 0.1% NP-40 (final concentration) for an
146 additional 3 minutes. Following centrifugation, the pellet was incubated in isotonic buffer (20 mM
147 Tris-HCl (pH 7.4), 150 mM KCl, 2 mM $MgCl_2$, 1 mM EGTA, 0.5 mM DTT, 0.5 mM PMSF) plus
148 0.1% NP-40 for another 3 minutes, then centrifuged. The resulting nuclear pellet was resuspended in
149 100 μl Benzonase®, 100U for 10 minutes at 37°C. RIPA buffer, 400 μl, was then added for 20 minutes
150 at room temperature (RT). Following centrifugation, the supernatant (nuclear soluble fraction) was
151 saved and the insoluble pellet, if present, was washed and resuspended in 100 μl Benzonase® 100 U.
152 Following a 10-minute digestion at 37°C, the digested lysate was combined with the nuclear soluble
153 fraction for immunoprecipitation, labeling with dibenzocyclooctyne (DBCO)-488, and Western blot
154 analysis.
155 DBCO labeling and immunoprecipitation were performed as follows. Prepared lysates were
156 heated at 95°C for 10 minutes to denature proteins and increase access to internal AHA-bearing
157 sequences. Iodoacetamide 10 mM, which decreases azide-independent labeling, was added to cooled
158 lysates for 30 minutes at RT (17). Lysates were then immunoprecipitated using anti-IL-2Rα antibody
159 directly conjugated magnetic beads. Conjugation was performed per manufacturer's instructions
160 (Click-&-Go, Click Chemistry Tools, Scottsdale, AZ). Following a 1h incubation at RT, beads (now

161 containing bound protein) were washed and incubated with 5 μM DBCO-488 (Click Chemistry Tools)
162 for 30 min at RT or overnight at 4°C. Beads were washed again and labeled protein was eluted with
163 lithium dodecyl sulfate (LDS) containing sample buffer in preparation for SDS-PAGE.
164 Levels of DBCO-labeled IL-2Rα were normalized using either total protein (Revert™ 700
165 Total Protein Stain) or total IL-2Rα detected by either the anti-IL-2Rα antibody from BosterBio or
166 anti-phospho-CD25 (ser268). The latter antibody was chosen for its strong signal and suggests that IL-
167 2Rα is active. A linear regression analysis was then performed on normalized levels of labeled IL-2Rα
168 and half-life was calculated via the following equation: $t_{1/2}$= ln(2)/slope of decay (13).
169
170 *Statistics*
171 Groups were compared using an unpaired, two-tailed t test with Welch's correction. P values in
172 figures are defined as follows: ns $P > 0.05$; * $P \leq 0.05$; ** $P \leq 0.01$; *** $P \leq 0.001$; **** $P \leq 0.0001$.
173
174 **Results**
175 *IL-2Rα KO VSMC express IL-2Rα protein*
176 To determine how IL-2Rα affects the function of VSMC, we isolated VSMC from IL-2Rα KO
177 and WT mice. WT and KO mice were genotyped using the protocol provided by JAX® (18). As a first
178 step following isolation and culture, we examined expression of IL-2Rα protein in WT and KO VSMC
179 by indirect immunofluorescence. VSMC isolated from WT mice expressed IL-2Rα primarily in the
180 nucleus, consistent with our recent observations in human VSMC (Figure 1A, B). However, IL-2Rα
181 was also detected in the nucleus of VSMC isolated from IL-2Rα KO mice. Similar results were
182 obtained with antibodies from multiple sources. Although most antibodies detected IL-2Rα in the
183 nucleus, two antibodies showed partial (Bioss) or predominantly (Genetex) membrane or cytoplasmic
184 localization (Figure 1A and Supplemental Figure 1). Although we have not established the reason
185 behind this differential detection, it likely relates to the fact that IL-2Rα is heavily glycosylated which
186 may obscure some epitopes. Preadsorption with a known peptide epitope, available for the antibody
187 obtained through BosterBio, abrogated staining (Figure 1C).
188 IL-2Rα KO mice were generated by replacing exons 2 and 3 of IL-2Rα with a neomycin
189 resistance gene (1). IL-2Rα is known to have multiple splice variants – three have been identified in
190 mouse IL-2Rα and nine in human IL-2Rα (19). To ensure that the IL-2Rα protein detected was not
191 produced by a splice variant, potentially excluding the neomycin resistance insert, we assessed the size
192 of IL-2Rα protein produced by WT and KO VSMC using Western blot analysis. As seen in Figure 1D,
193 WT and IL-2Rα KO VSMC expressed IL-2Rα of the same size, identical to that of human VSMC and
194 Jurkat T cells (9). These results suggest that IL-2Rα KO VSMC express full-length IL-2Rα.
195
196 *IL-2Rα KO splenocytes express IL-2Rα protein*
197 Because IL-2Rα expression and function are mainly studied in T cells, we asked whether
198 lymphocytes from IL-2Rα KO mice express IL-2Rα protein. To this end, we isolated splenocytes from
199 WT and IL-2Rα KO mice and examined IL-2Rα expression by flow cytometry in the presence or
200 absence of stimulation with phytohemagglutinin (PHA) to upregulate membrane IL-2Rα. Since IL-
201 2Rα appears mainly localized to the nucleus in VSMC, we also permeabilized cells to look for nuclear
202 expression. To assess IL-2Rα expression, we used two of the same antibodies used in VSMC, sourced
203 from Genetex and BosterBio (see Figure 1).
204 In non-permeabilized cells, a subset of WT splenocytes expressed IL-2Rα on their cell surface
205 when stimulated with PHA (Figure 2A). A small subset of KO cells also expressed IL-2Rα. Upon
206 permeabilization, however, IL-2Rα was detected by in the majority of WT splenocytes (70-80%). IL-
207 2Rα was also detected in permeabilized KO splenocytes, however the frequency was lower than in WT

208 cells, particularly those stained with the anti-IL-2Rα from Genetex. The intensity of staining was also
209 decreased in permeabilized KO vs WT splenocytes (Figure 2B). Although not statistically significant,
210 the frequency of permeabilized cells expressing nuclear IL-2Rα was decreased in WT cells stimulated
211 with PHA vs those that were unstimulated. These results are consistent with our finding that, in
212 VSMC, nuclear IL-2Rα is decreased in proliferating vs quiescent cells (unpublished observation).
213 These results suggested that IL-2Rα could be localized to the nucleus in lymphocytes. To
214 address this question, we separated splenocyte lysates into membrane, cytoplasm, and nuclear
215 fractions. Consistent with our findings in VSMC, IL-2Rα was present in the nucleus (Figure 2C).
216 We then asked whether a commonly used anti-IL-2Rα antibody, rat anti-mouse IL-2Rα clone
217 PC61.5, would yield similar results (20–23). Non-permeabilized WT splenocytes stimulated with PHA
218 yielded strong expression, as expected, and similarly treated KO cells were negative (Figure 3A).
219 However, permeabilization yielded only low levels of IL-2Rα in WT cells and KO cells were negative.
220 Given the nuclear localization of IL-2Rα (Figures 1,2), we reasoned that a potential association with
221 DNA might be blocking some epitopes. To test this question, we digested permeabilized cells with
222 Benzonase®, a genetically engineered endonuclease that degrades all forms of DNA and RNA. IL-2Rα
223 was strongly detected in permeabilized WT and KO splenocytes following Benzonase® digestion,
224 although the level of expression per cell (mean channel fluorescence) was much higher in WT cells
225 (Figure 3B). Pre-adsorption of PC61.5 with purified mouse IL-2Rα protein abrogated this staining
226 (Figure 3A).
227 Although prior attempts at using clone PC61.5 to detect IL-2Rα in VSMC yielded poor results,
228 based on the above findings we digested methanol-fixed VSMC with Benzonase®. Digestion of mouse
229 VSMC with Benzonase® allowed for the detection of IL-2Rα in the nucleus, consistent with our
230 findings in T cells (Figure 3C). In addition, these results suggest that at least a portion of nuclear IL-
231 2Rα binds DNA.
232
233 *Genomic sequencing demonstrates IL-2RA deletion*
234 In light of our results demonstrating that both IL-2Rα KO splenocytes and VSMC produce IL-
235 2Rα, we sought to establish its source. As a first step, we asked if the deletion in the *IL2RA* gene was
236 intact. To this end, we sequenced genomic DNA isolated from WT and KO VSMC. Targeted genome
237 sequencing of the *IL2RA* gene from KO cells revealed correct deletion of exons 2 and 3 as initially
238 reported by Willerford, et al (1) (Figure 4).
239
240 *Multiple tissues in IL-2Rα KO mice have low levels of the IL-2RA gene*
241 Given that *IL2RA* was correctly deleted, we considered other sources of the WT gene. One
242 potential source of the WT *IL2RA* gene is maternal transfer. Maternal microchimerism, the transfer of
243 cells from mother to fetus, is well established in humans and mice wherein maternal DNA/cells can
244 persist for decades in offspring (24–28). Because IL-2Rα KO mice are infertile, they are generated by
245 mating IL-2Rα heterozygotes; consequently, heterozygous maternal cells are likely present in IL-2Rα
246 KO mice. Maternal microchimerism may therefore represent result a potential source of IL-2Rα in KO
247 offspring of heterozygous females. Our laboratory previously demonstrated that maternal
248 microchimerism was responsible for the presence of IL-2 in IL-2 KO mice, which obscured severe
249 defects in thymic development (27).
250 Using the *IL2RA* gene as an indicator of maternal microchimerism, we extracted genomic DNA
251 from IL-2Rα KO tissues and looked for evidence of *IL2RA*, using primers that amplify a segment
252 within exon 2 that should be absent in KO mice (1). Relative levels of *IL2RA* were assessed by qPCR
253 of genomic DNA. QPCR of maternal markers in genomic DNA of offspring has been used by other
254 investigators to detect maternal microchimerism (24). As seen in Figure 5A, 6/6 spleens, 6/6 kidneys,

255 and 3/3 hearts from adult KO mice had detectable (RQ > 0 with one of the KO spleens as reference)
256 levels of *IL2RA*. As further evidence for the presence of maternal cells in offspring of IL-2Rα het
257 breeders, we assessed spleens from IL-2Rα WT offspring of heterozygous parents for the neomycin
258 resistance gene used in the generation of IL-2Rα KO mice. Five of five spleens tested had detectable
259 levels of the *NeoR* gene (Figure 5B). As expected, control spleens from unrelated mice that were not
260 offspring of IL-2Rα het mice had no detectable *NeoR* gene.
261
262 *G418 decreases IL-2Rα protein expression in IL-2Rα KO VSMC*
263 As previously mentioned, IL-2Rα KO mice were generated by replacing exons 2 and 3 of IL-
264 2Rα with a neomycin resistance gene insert as a selectable marker (1). If IL-2Rα KO VSMC contained
265 low numbers of IL-2Rα heterozygous cells, as our results suggest, then treatment with neomycin might
266 eliminate these cells if they are less resistant to neomycin than KO cells. In turn, IL-2Rα protein
267 expression should decrease. To test this hypothesis, we cultured WT and KO VSMC with increasing
268 concentrations of G418 (a neomycin analog). G418 nearly eliminated WT cells at a concentration of 2
269 mg/ml (Figure 6A). However, many VSMC isolated from KO mice survived this treatment. IL-2Rα
270 production by these cells following treatment with G418 was significantly diminished compared to
271 untreated VSMC isolated from IL-2Rα KO mice as shown by both immunofluorescence and Western
272 blot analysis (Figure 6A, C). These data suggest that the neomycin resistance protein is expressed and
273 functional in IL-2Rα KO VSMC, and that treatment of KO VSMC with G418 decreased IL-2Rα
274 protein originating from heterozygous cells.
275
276 *IL-2Rα protein is transferred between cells*
277 Although our first attempt at clearance of IL-2Rα protein by treatment with G418 significantly
278 decreased IL-2Rα protein expression, we were unable to eliminate IL-2Rα despite ongoing treatment
279 with G418 and/or increased dosage (Figure 7). Upon performing formal kill curves with G418, we
280 observed that the difference in resistance between heterozygous and homozygous cells is probably not
281 large enough to differentially eliminate all heterozygous cells (Supplemental Figure 2).
282 As part of efforts to identify the source of ongoing IL-2Rα production, we noted that VSMC
283 were heterogeneous in size, and that large cells appeared to express high levels of IL-2Rα protein
284 (Figure 7A). Using filters (Pluriselect, Leipzig, Germany), we separated cells into those that passed
285 through a 1 micron filter from the remainder that did or did not pass through a 30 micron filter. We
286 then compared levels of *IL2RA* DNA amongst these cells and with those that had not received G418.
287 As seen in Figure 7B, larger cells contained relatively more *IL2RA* DNA than smaller cells, and those
288 without G418 treatment contained the most *IL2RA* DNA, consistent with our observations of IL-2Rα
289 protein expression (Figures 6,7).
290 Given the above findings, combined with our observation that most VSMC isolated from IL-
291 2Rα KO mice expressed at least low levels of IL-2Rα protein, we asked whether IL-2Rα could be
292 transferred between cells. To this end, we co-cultured IL-2Rα KO VSMC with human VSMC using a
293 transwell insert, in which human VSMC were suspended over KO VSMC and separated by a filter. We
294 chose human VSMC for their robust IL-2Rα protein expression (Figure 1). IL-2Rα was easily
295 detectable in IL-2Rα KO VSMC that had been co-cultured with human VSMC, compared to those that
296 were not (Figure 7C). These results suggest that IL-2Rα protein is transferred between cells by a
297 means not requiring cell contact, likely through extracellular vesicles such as exosomes or apoptotic
298 bodies.
299
300
301

302 *Half-life of IL-2Rα*
303 While the previous results suggest that IL-2Rα protein present in KO mice originated from
304 maternal microchimerism, the low levels of *IL2RA* DNA detected did not seem consistent with the
305 comparatively high levels of protein. One way in which protein levels may be regulated is through
306 their half-life. In a recent report by Chen, et al, a systematic study of half-lives of proteins in human
307 HepG2 cells showed that most proteins had half-lives ranging from 4-14 hours (29).
308 Given the easily detectable IL-2Rα protein evident in KO mice, we hypothesized that the half-
309 life of IL-2Rα is long, likely days versus hours. To measure the half-life of IL-2Rα, we performed a
310 pulse chase experiment, in which we labeled newly synthesized proteins with a methionine analog,
311 AHA, then assessed their degradation over time through loss of labeled proteins. Incorporated AHA
312 was detected by fluorescently labeled DBCO, which binds the azido group in AHA through strain
313 promoted alkyne-azide cycloaddition, a copper-free click reaction (14). Based on our results showing
314 that IL-2Rα is localized primarily to the nucleus, we focused on the nuclear fraction. IL-2Rα protein
315 was isolated by immunoprecipitation using the anti-IL-2Rα from BosterBio, and then detected with
316 either the anti-IL-2Rα from BosterBio or an anti-IL-2Rα (phospho-ser 268). Levels of DBCO-labeled
317 IL-2Rα, assessed by densitometry, were normalized based on either total protein or total IL-2Rα
318 protein per band. Normalizing with total IL-2Rα protein was sometimes difficult since the DBCO label
319 variably impacted recognition of IL-2Rα (Supplemental Figure 3). Based on 3 separate experiments,
320 the half-life of IL-2Rα was 8.4 ± 2.5 days (Figure 8). These results demonstrate that the half-life of IL-
321 2Rα is longer than most cellular proteins and may explain the discrepancy between levels of *IL2RA*
322 DNA and protein observed in IL-2Rα KO mice.
323
324 *IL-2Ra KO VSMC*
325 Responses of IL-2Rα KO VSMC to sera, evident in routine culture, began to give us insight
326 into the differences between WT and KO VSMC. Doubling times were significantly shorter in KO vs
327 WT VSMC (Figure 9). KO VSMC were also much smaller than WT and took up less DAPI; these
328 differences were heightened upon stimulation with FBS (Figure 9). The latter observations are
329 consistent with the finding that DNA content is directly proportional to cell size (30). In comparing
330 nuclear area and DNA content of WT and KO VSMC, however, we noted that the decrease in DNA
331 content was out of proportion to the decrease in nuclear area. KO nuclei were approximately half the
332 size of WT, but only had 1/6 the amount of DNA. This finding suggests that KO VSMC are
333 hypodiploid, which implies a severe dysregulation of cell proliferation and/or division. Hypodiploid
334 cells are mainly associated with an aggressive form of acute lymphoblastic leukemia (31,32).
335
336 **Discussion**
337 Knock out mice are often used to determine the function of a protein. Both IL-2 and IL-2Rα
338 KO mice were instrumental in determining that the IL-2/IL-2R system plays a major regulatory role in
339 the immune system by promoting the survival of T regulatory cells and through activation-induced cell
340 death (1,3,33). Our results show that IL-2Rα is diminished, but not absent, in IL-2Rα KO mice.
341 Furthermore, our data suggest that the source of IL-2Rα is maternal microchimerism. The infertility of
342 IL-2Rα KO mice, mandating a heterozygous mother, combined with the long half-life of IL-
343 2Rα, creates a unique situation in which substantial amounts of IL-2Rα are present in KO mice. The
344 predominantly nuclear localization of IL-2Rα, reported here, is likely responsible for its lack of
345 detection before now.
346 Our studies of IL-2Rα KO mice and the mechanisms contributing to its incomplete elimination
347 have led to several remarkable discoveries including: (1) IL-2Rα is localized primarily to the nucleus,
348 (2) IL-2Rα protein has a long half-life, and (3) IL-2Rα is transmitted between cells. First, and

349 foremost, is our observation that IL-2Rα is localized primarily to the nucleus. Prior reports addressing
350 the potential nuclear localization of IL-2R subunits are rare. In 1988, Jothy, et al showed that IL-2Rα
351 was transiently localized to the nucleus of concanavalin A supernatant-stimulated HT-2 cells (34).
352 Conversely, Fujii, et al, showed that neither IL-2Rβ nor IL-15Rα could be transported to the nucleus,
353 however they did not test IL-2Rα (35). Our report adds to this literature, clearly demonstrating that IL-
354 2Rα localizes to the nucleus. In this location, our data show that IL-2Rα deficient cells become
355 smaller and lose DNA when stimulated to proliferate. These results are consistent with our finding that
356 quiescent and senescent cells have increased nuclear IL-2Rα relative to proliferating cells (unpublished
357 observation). While not formally studied, our methods also intimate that IL-2Rα binds DNA, given
358 that we were unable to immunoprecipitate IL-2Rα without first digesting DNA. Taken together, these
359 findings suggest that that IL-2Rα contributes to the regulation of cell division and/or acts as a
360 transcription factor.
361 In addition to its nuclear localization, we have also determined that IL-2Rα has a long half-life
362 relative to most proteins. Systemic studies of protein half lives in cells and tissues have shown that
363 mitochondrial and nuclear proteins have the longest half-lives, consistent with the predominantly
364 nuclear localization of IL-2Rα reported here (29,36). Proteins with long half-lives tend to play key
365 structural or functional roles within cells. Histones, for example, with half-lives ranging from 15 days
366 in dividing cells to 240+ in non-dividing cells, contribute to the organization of chromatin which in
367 turn regulates cell division, DNA damage responses, gene expression, and cell fate (29,37,38). Several
368 mitochondrial proteins have half-lives on the order of 7 days; these longer-lived proteins were found to
369 contribute to the stability of the electron transport chain (39). The long half-life of IL-
370 2Rα, demonstrated here, provides additional support to the concept that IL-2Rα has a newfound,
371 fundamental role in regulating cell size and proliferation.
372 Finally, our investigation into the incomplete elimination of IL-2Rα mice revealed that IL-2Rα
373 is shared/transported between cells. Given that cell contact was not required for this transmission, it is
374 likely that IL-2Rα was transported through extracellular vesicles such as an exosomes or apoptotic
375 bodies. Extracellular vesicles are a major means of intercellular communication and have been shown
376 to participate in many biological processes including differentiation, proliferation, apoptosis, motility,
377 and others (40). If IL-2Rα plays a cell intrinsic role in regulating proliferation, as suggested by our
378 findings, then transmission of IL-2Rα by its "producers" may promote the normal function of
379 surrounding KO cells and attenuate the consequences of IL-2Rα deficiency.
380 As previously described, we used G418 resistance to decrease the production of IL-2Rα,
381 originating from IL-2Rα heterozygous cells, in VSMC isolated from IL-2Rα KO mice. This method
382 was partially successful (Figures 6,7); however, to date we have not been able to completely eradicate
383 IL-2Rα. Reasons for this ongoing incomplete eradication likely include (1) insufficient difference
384 between G418 resistance of homozygous vs heterozygous cells, (2) lack of means to detect and
385 exclude live IL-2Rα producing cells, and (3) techniques such as clonal dilution are challenging in
386 primary VSMC as their viability at the single cell level is poor. Our laboratory is in the process of
387 finding other methods of detecting and eliminating IL-2Rα producing cells to establish a complete IL-
388 2Rα KO phenotype both *in vitro* and *in vivo*.
389 In summary, our data reveals the surprising finding that IL-2Rα KO mice express significant
390 amounts of IL-2Rα protein. Our initial assessment of IL-2Rα KO VSMC suggests that IL-2Rα,
391 localized to the nucleus and independent of IL-2, plays an unexpected role in the regulation of cell
392 proliferation.
393
394
395

## Conflict of Interest

The authors declare that the research was conducted in the absence of any commercial or financial relationships that could be construed as a potential conflict of interest.

## Author Contributions

VW, KD, and GC performed experiments, analyzed data and contributed to experimental design. LW designed experiments, analyzed data, and wrote the manuscript. All authors critically reviewed and edited the manuscript.


## Funding

These studies were supported by a grant from the National Institutes of Health (R03AG068696) and from the Boonshoft School of Medicine at Wright State University to LW.

## Acknowledgements

The authors would like to extend a heartfelt thanks to the Microarray and Microbiome Sequencing Core Facility at University of Texas Southwestern Medical Center for performing the quantitative PCR experiments and targeted genomic sequencing assay for the present study.


## References


1. Willerford DM, Chen J, Ferry JA, Davidson L, Ma A, Alt FW. Interleukin-2 receptor alpha chain regulates the size and content of the peripheral lymphoid compartment. Immunity. 1995 Oct;3(4):521–30.
2. Malek TR, Castro I. Interleukin-2 receptor signaling: at the interface between tolerance and immunity. Immunity. 2010 Aug;33(2):153–65.
3. Toomer KH, Lui JB, Altman NH, Ban Y, Chen X, Malek TR. Essential and non-overlapping IL-2Rα-dependent processes for thymic development and peripheral homeostasis of regulatory T cells. Nat Commun. 2019;10(1037).
4. Sharma R, Zheng L, Deshmukh US, Jarjour WN, Sung SJ, Fu SM, et al. Cutting Edge: A Regulatory T Cell-Dependent Novel Function of CD25 (IL-2Rα) Controlling Memory CD8+ T Cell Homeostasis. J Immunol. 2007 Feb 1;178(3):1251–5.
5. Sharma R, Bagavant H, Jarjour WN, Sung S-SJ, Ju S-T. The Role of Fas in the Immune System Biology of IL-2Rα Knockout Mice: Interplay among Regulatory T Cells, Inflammation, Hemopoiesis, and Apoptosis. J Immunol. 2005 Aug 1;175(3):1965–73.
6. García de Galdeano A, Boyano D, Smith-Zubiaga I, Cañavate L. B16F10 Murine Melanoma Cells Express Interleukin-2 and a Functional Interleukin-2 Receptor. Tumor Biol. 1996 Mar 1;17(3):155–67.
7. Kronin V, Vremec D, Shortman K. Does the IL-2 receptor alpha chain induced on dendritic cells have a biological function? Int Immunol. 1998 Feb 1;10(2):237–40.
8. Von Bergwelt-Baildon MS, Popov A, Saric T, Chemnitz J, Classen S, Stoffel MS, et al. CD25 and indoleamine 2,3-dioxygenase are up-regulated by prostaglandin E2 and expressed by tumor-associated dendritic cells in vivo: additional mechanisms of T-cell inhibition. Blood. 2006 Jul 1;108(1):228–37.
9. Arumugam P, Carroll KL, Berceli SA, Barnhill S, Wrenshall LE. Expression of a Functional IL-2 Receptor in Vascular Smooth Muscle Cells. J Immunol. 2019 Feb 1;202(3):694–703.
10. Kwartler C, Zhou P, Kuang S-Q, Duan X-Y, Gong L, Milewicz D. Vascular Smooth Muscle Cell Isolation and Culture from Mouse Aorta. BIO-PROTOCOL. 2016;6(23).
11. Libby P, O'Brien K V. Culture of quiescent arterial smooth muscle cells in a defined serum-free

445 medium. J Cell Physiol. 1983 May;115(2):217–23.
446 12. Protocol 22371 - Il2ra<tm1Dw> [Internet]. The Jackson Laboratory. [cited 2023 Nov 1].
447 Available from: https://www.jax.org/Protocol?stockNumber=002952&protocolID=22371
448 13. Morey TM, Esmaeili MA, Duennwald ML, Rylett RJ. SPAAC Pulse-Chase: A Novel Click
449 Chemistry-Based Method to Determine the Half-Life of Cellular Proteins. Front Cell Dev Biol.
450 2021;9(722560).
451 14. Lutz J-F. Copper-Free Azide-Alkyne Cycloadditions: New Insights and Perspectives. Angew
452 Chem IntEd. 2008;47:2182–4.
453 15. Agard NJ, Prescher JA, Bertozzi CR. A strain-promoted [3 + 2] azide-alkyne cycloaddition for
454 covalent modification of biomolecules in living systems. J Am Chem Soc. 2004 Nov
455 24;126(46):15046–7.
456 16. Senichkin V, Prokhorova E, Zhivotovsky B, Kopeina G. Simple and Efficient Protocol for
457 Subcellular Fractionation of Normal and Apoptotic Cells. Cells. 2021;10(852):1–13.
458 17. Van Geel R, Pruijn GJM, Van Delft FL, Boelens WC. Preventing thiol-yne addition improves
459 the specificity of strain-promoted azide-alkyne cycloaddition. Bioconjug Chem.
460 2012;23(3):392–8.
461 18. 002952 - IL-2Rα[-] Strain Details [Internet]. The Jackson Laboratory. [cited 2023 Sep 30].
462 Available from: https://www.jax.org/strain/002952
463 19. Thierry-Meig J, Thierry-Meig D. AceView: a comprehensive cDNA-supported gene and
464 transcripts annotation. Genome Biol. 2006;7:S12.
465 20. McHugh RS, Shevach EM. Cutting Edge: Depletion of CD4+CD25+ Regulatory T Cells Is
466 Necessary, But Not Sufficient, for Induction of Organ-Specific Autoimmune Disease. J
467 Immunol. 2002 Jun 15;168(12):5979–83.
468 21. Setiady YY, Coccia JA, Park PU. In vivo depletion of CD4+FOXP3+ Treg cells by the PC61
469 anti-CD25 monoclonal antibody is mediated by FcγRIII+ phagocytes. Eur J Immunol.
470 2010;40(3):780–6.
471 22. Kraft ARM, Wlodarczyk MF, Kenney LL, Selin LK. PC61 (anti-CD25) treatment inhibits
472 influenza A virus-expanded regulatory T cells and severe lung pathology during a subsequent
473 heterologous lymphocytic choriomeningitis virus infection. J Virol. 2013 Dec;87(23):12636–47.
474 23. Solomon I, Amann M, Goubier A, Arce Vargas F, Zervas D, Qing C, et al. CD25-Treg-
475 depleting antibodies preserving IL-2 signaling on effector T cells enhance effector activation
476 and antitumor immunity. Nat cancer. 2020 Dec 1;1(12):1153.
477 24. Su E, Johnson K, Tighioart H, Bianchi D. Murine maternal cell microchimerism: analysis using
478 real-time PCR and in vivo imaging. Biol Reprod. 2008;78(5):883–7.
479 25. Stelzer IA, Thiele K, Solano ME. Maternal microchimerism: Lessons learned from murine
480 models. J Reprod Immunol. 2015;108:12–25.
481 26. Schepanski S, Chini M, Sternemann V, Urbschat C, Thiele K, Sun T, et al. Pregnancy-induced
482 maternal microchimer-ism shapes neurodevelopment and behavior in mice. Nat Commun.
483 2022;13(4571).
484 27. Wrenshall LE, Stevens ET, Smith DR, Miller JD. Maternal microchimerism leads to the
485 presence of interleukin-2 in interleukin-2 knock out mice: Implications for the role of
486 interleukin-2 in thymic function. Cell Immunol. 2007;245(2):80–90.
487 28. Dutta P, Molitor-Dart M, Bobadilla JL, Roenneburg DA, Yan Z, Torrealba JR, et al.
488 Microchimerism is strongly correlated with tolerance to noninherited maternal antigens in mice.
489 Blood. 2009;114(17):3578–87.
490 29. Chen W, Smeekens JM, Wu R. Systematic study of the dynamics and half-lives of newly
491 synthesized proteins in human cells. Chem Sci. 2016;7:1393–400.
492 30. Gillooly JF, Hein A, Damiani R. Nuclear DNA content varies with cell size across human cell

types. Cold Spring Harb Perspect Biol. 2015;7(7):1–27.
31. Safavi S, Forestier E, Golovleva I, Barbany G, Nord KH, Moorman A V., et al. Loss of chromosomes is the primary event in near-haploid and low-hypodiploid acute lymphoblastic leukemia. Leukemia. 2013;27(1):248–50.
32. Safavi S, Paulsson K. Near-haploid and low-hypodiploid acute lymphoblastic leukemia: Two distinct subtypes with consistently poor prognosis. Blood. 2017;129(4):420–3.
33. Kundig T, Schorle H, Bachmann M, Hengartner H, Zinkernagel R, Horak I. Immune responses in interleukin-2-deficient mice. Science (80- ). 1993;262(5136):1059–61.
34. Jothy S, Abadie A, Froussard P, Duphot M, Thèze J. Nuclear location of the p55 subunit of the IL-2 receptor following activation of the HT-2 T helper cell line. Ann Inst Pasteur Immunol. 1988;139(3):237–44.
35. Fujii H, Hoshino A. Lack of nuclear translocation of cytoplasmic domains of IL-2/IL-15 receptor subunits. Cytokine. 2008;46(3):302–8.
36. Price JC, Guan S, Burlingame A, Prusiner SB, Ghaemmaghami S. Analysis of proteome dynamics in the mouse brain. Proc Natl Acad Sci. 2010;107:14508–13.
37. Mathieson T, Franken H, Kosinski J, Kurzawa N, Zinn N, Sweetman G, et al. Systematic analysis of protein turnover in primary cells. Nat Commun. 2018;9(689).
38. Shmueli MD, Sheban D, Eisenberg-Lerner A, Merbl Y. Histone degradation by the proteasome regulates chromatin and cellular plasticity. FEBS J. 2022;289(12):3304–16.
39. Krishna S, Arrojo Drigo R, Capitanio JS, Ramachandra R, Ellisman M, Hetzer MW. Identification of long-lived proteins in the mitochondria reveals increased stability of the electron transport chain. Dev Cell. 2021;56(21):2952–65.
40. Liu Y-J, Wang C. REVIEW Open Access A review of the regulatory mechanisms of extracellular vesicles-mediated intercellular communication. Cell Commun Signal. 2023;21:77.
41. Roth V. Doubling Time Calculator [Internet]. 2006. Available from: https://www.doubling-time.com/compute_more.php

521 **Figure Legends**

522 **Figure 1. VSMC isolated from IL-2Rα KO mice express IL-2Rα protein.** (A) VSMC, isolated
523 from IL-2Rα WT and KO mice, were cultured to 60 - 70% confluency. After fixation and blocking,
524 primary antibodies recognizing IL-2Rα, purchased from various sources as indicated, were applied to
525 VSMC followed by the appropriate Cy5 conjugated secondary. Cells were imaged using an EVOS FL
526 epifluorescence microscope (ThermoFisher Scientific). Scale bar = 100 μ. (B) Human VSMC were
527 stained with the anti-IL-2Rα from BosterBio. Scale bar = 100 μ. (C) Murine VSMC were stained as in
528 (A) using anti-IL-2Rα from Boster with/without pre-adsorption with immunizing peptide. Scale bar =
529 200 μ. (D) Lysates of VSMC or Jurkat T cells were separated by SDS-PAGE and analyzed for
530 expression of IL-2Rα, using anti-IL-2Rα from Boster. Histone H3 was used as a loading control.
531 Results shown are representative of >5 (A,B), 3 (C), and >5 (D) separate experiments.
532

533 **Figure 2. IL-2Rα is detectable in the nucleus of IL-2Rα WT and KO splenocytes.**
534 (A) Splenocytes, prepared fresh or following 48h of stimulation with PHA 1 μg/ml, were stained with
535 anti-IL-2Rα antibodies or isotype controls as indicated with/without first permeabilizing via methanol.
536 Graphs to the right of histograms represent a summary of individual values from multiple experiments.
537 (B) represents the average MFIs ± SEM, derived from (A), of permeabilized splenocytes stained with
538 anti-IL-2Rα antibodies as indicated. (C) Splenocytes were stimulated with PHA for 48h, pelleted and
539 fractionated into membrane, cytoplasm, and nuclear fractions, then analyzed by Western blot probing
540 with antibodies as indicated. Blots represent lysates processed in parallel. Total protein, obtained from
541 stain-free gels (Bio-Rad), shows the single most prominent band present across all samples. Results
542 shown are representative of ≥ 3 experiments.
543

544 **Figure 3. IL-2Rα is detected in permeabilized splenocytes by rat anti-mouse IL-2Rα (clone PC**
545 **61) following DNA digestion.** (A) Splenocytes were prepared as described in Figure 2. A subset of
546 methanol permeabilized cells were treated with Benzonase® 250U/$10^6$ cells or enzyme buffer for 50
547 minutes at 37°C prior to staining. In a subset of samples, anti-IL-2Rα/clone PC 61 was pre-adsorbed
548 with an excess of purified mouse IL-2Rα. Graphs to the right of histograms represent a summary of
549 individual values from multiple experiments. "Block" indicates use of pre-adsorbed anti-IL-2Rα. (B)
550 represents the average MFIs ± SEM, derived from (A), of permeabilized splenocytes treated with
551 Benzonase®. (C) VSMC were permeabilized with methanol and treated with Benzonase® or buffer, as
552 indicated above, then stained with anti-IL-2Rα/clone PC 61. Note that digestion with Benzonase®
553 eliminates DAPI staining as expected. Scale bar = 100 μ.
554

555 **Figure 4. Exons 2 and 3 of IL-2Rα gene are deleted in IL-2Rα KO mice.**
556 Genomic DNA isolated from WT and KO VSMC underwent targeted sequencing, with a focus on the
557 IL-2Rα locus. Exons 2 and 3 of IL-2Rα are deleted as reported by Willerford, et al (1).
558

559 **Figure 5. IL-2Rα gene is present in IL-2Rα KO tissues.** Genomic DNA was isolated from various
560 organs as indicated. Levels of *IL2RA* (A) or *Neo* resistance (B) DNA were measured in each tissue by
561 qPCR. The relative quantity (RQ) of IL-2Rα or NeoR DNA was measured relative to a single KO
562 spleen (A) or a WT spleen (B).
563

564 **Figure 6. G418 decreases IL-2Rα protein expression in VSMC isolated from IL-2Rα KO mice.**
565 (A) VSMC, isolated from IL-2Rα WT and KO mice, were cultured in the presence/absence of G418 at
566 2 mg/ml. Cells were probed for IL-2Rα expression using the anti-IL-2Rα from Boster as described in
567 Figure 1. Scale bar = 400 μ. (B) The intensity of IL-2Rα staining in all cells from (A) was measured in

568 an image cytometer and converted to a histogram using flow cytometry software. (C) KO VSMC,
569 cultured as described in A, were lysed. Extracted proteins were separated by SDS-PAGE and analyzed
570 by Western blot for expression of IL-2Rα using the anti-IL-2Rα antibody from Boster. Intensity of the
571 IL-2Rα band from each treatment was expressed as a ratio of IL-2Rα/histone H3. Densitometry was
572 performed using Image Lab software from Bio-Rad Laboratories. Results shown for A,C are
573 representative of >3,2 separate experiments respectively.
574
575 **Figure 7. IL-2Rα is transferred between cells.** (A) VSMC were cultured for 96h with increasing
576 concentrations of G418 as indicated. IL-2Rα protein expression was detected using the anti-IL-
577 2Rα antibody from BosterBio. (B) VSMC, cultured in G418, were separated by size using 1 and 30
578 micron filters as indicated. Genomic DNA was isolated from cell pellets and levels of *IL2RA* DNA
579 were quantified relative to the 1 micron cells. (C) Human VSMC were placed in transwell inserts and
580 co-cultured with murine VSMC for 96h and compared to murine VSMC without co-culture. IL-
581 2Rα protein expression was detected using the anti-IL-2Rα antibody from BosterBio. Intensity of IL-
582 2Rα staining in all cells was measured in an image cytometer (Cytation) then converted to a histogram
583 or bar graph using flow cytometry or data analysis software. Scale bar = 200 μ.
584
585 **Figure 8. IL-2Rα exhibits a prolonged half-life.** VSMC were labeled with AHA-containing,
586 methionine free media for 48h then chased with complete media for the durations above. IL-2Rα was
587 then isolated by immunoprecipitation with anti-IL-2Rα from BosterBio. AHA-labeled IL-2Rα was
588 detected by DBCO-488 and total IL-2Rα was detected using anti-IL-2Rα, anti-phospho IL-
589 2Rα ser268, or total protein stain as indicated. DBCO intensities, normalized to total IL-2Rα, were
590 graphed on a linear scale and linear regression analysis was performed to determine the protein half-
591 life. Blots at the left and right edges of the figure show VSMC fractionated into membrane, soluble
592 nuclear, and insoluble nuclear fractions (both nuclear fractions digested with Benzonase®) and probed
593 with antibodies as indicated. Circled lanes indicate the fractions that were combined for
594 immunoprecipitation. The half-life on the left hand side of the figure was calculated using the band
595 detected by anti-phospho IL-2Rα ser268 and total protein (of that band) for normalization. The half-
596 life on the right hand side was calculated using the band detected by anti-IL-2Rα from BosterBio and
597 immunodetection for normalization. In the above experiments, immunoprecipitated IL-2Rα was eluted
598 using a denaturing buffer. Use of a non-denaturing buffer yielded a similar half-life of 8.25 days.
599
600 **Figure 9. IL-2Rα KO VSMC are small and hypodiploid.** (A) VSMC, isolated from IL-2Rα WT and
601 KO mice, were cultured for 72h in serum free media with increasing concentrations of FBS. Cells were
602 probed for IL-2Rα expression using the anti-IL-2Rα from Boster as described in Figure 1. Scale bar =
603 200 μ. (B) Doubling times of WT and KO VSMC were calculated using three time points over 72h
604 (41). Data represent average ± SEM of 5 separate experiments. (C, top) Phase and IL-2Rα overlay
605 images from WT and KO VSMC in serum free media and probed for IL-2Rα as in (A). Scale bar =
606 100 μ. (C, middle and bottom) Nuclei of VSMC from (A) were imaged for area and DAPI intensity
607 using a Cytation imaging plate reader (Biotek). Data accrued from these images were then processed
608 using flow cytometry software. Results shown are representative of 3(A,C) separate experiments or 5
609 (B) collated experiments.
610
611
612

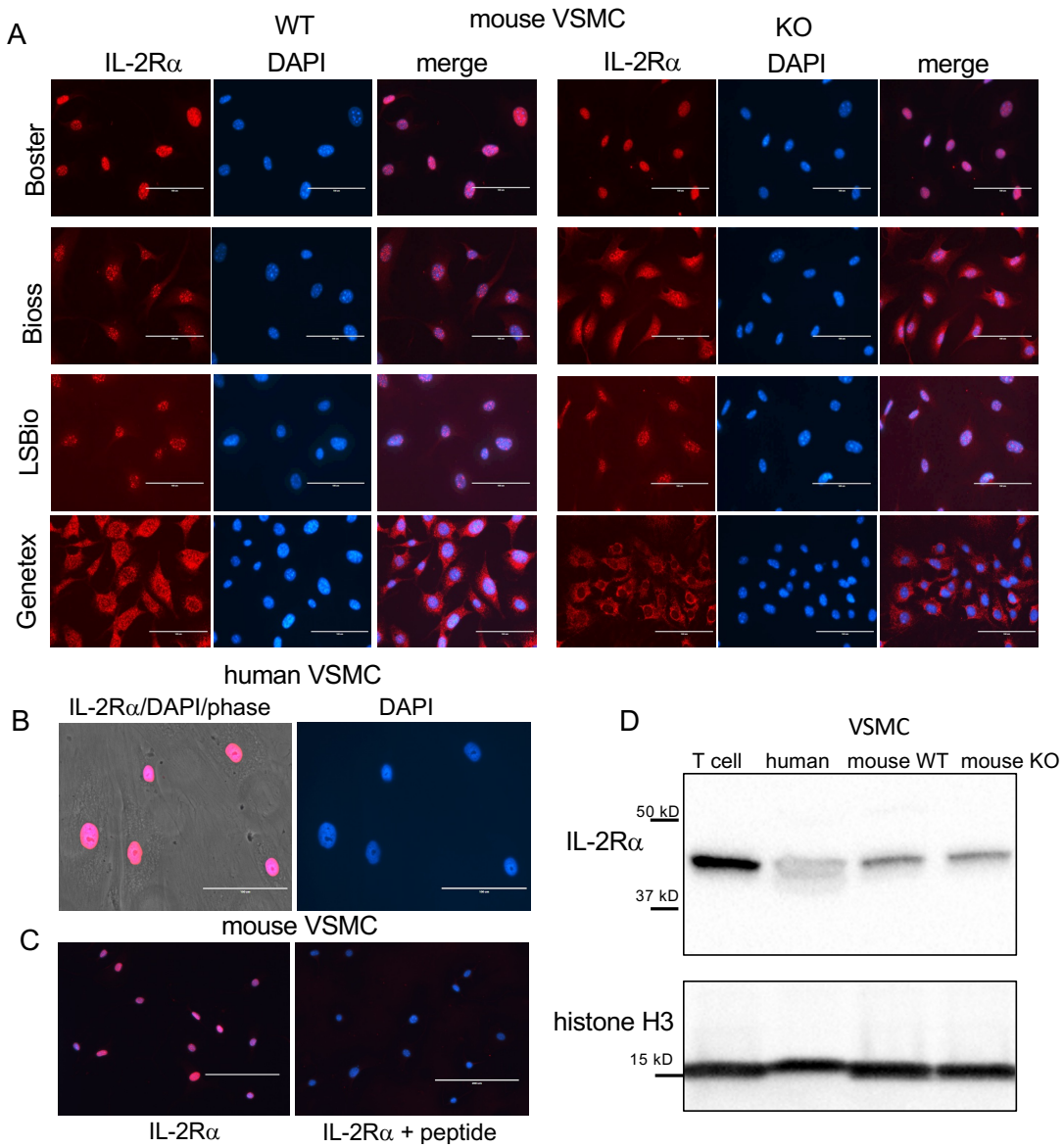
A
mouse VSMC
WT
KO
IL-2Rα
DAPI
merge
IL-2Rα
DAPI
merge
Boster
Bioss
LSBio
Genetex
human VSMC
B
IL-2Rα/DAPI/phase
DAPI
C
mouse VSMC
IL-2Rα
IL-2Rα + peptide
D
VSMC
T cell
human
mouse WT
mouse KO
50 kD
IL-2Rα
37 kD
histone H3
15 kD

Figure 1

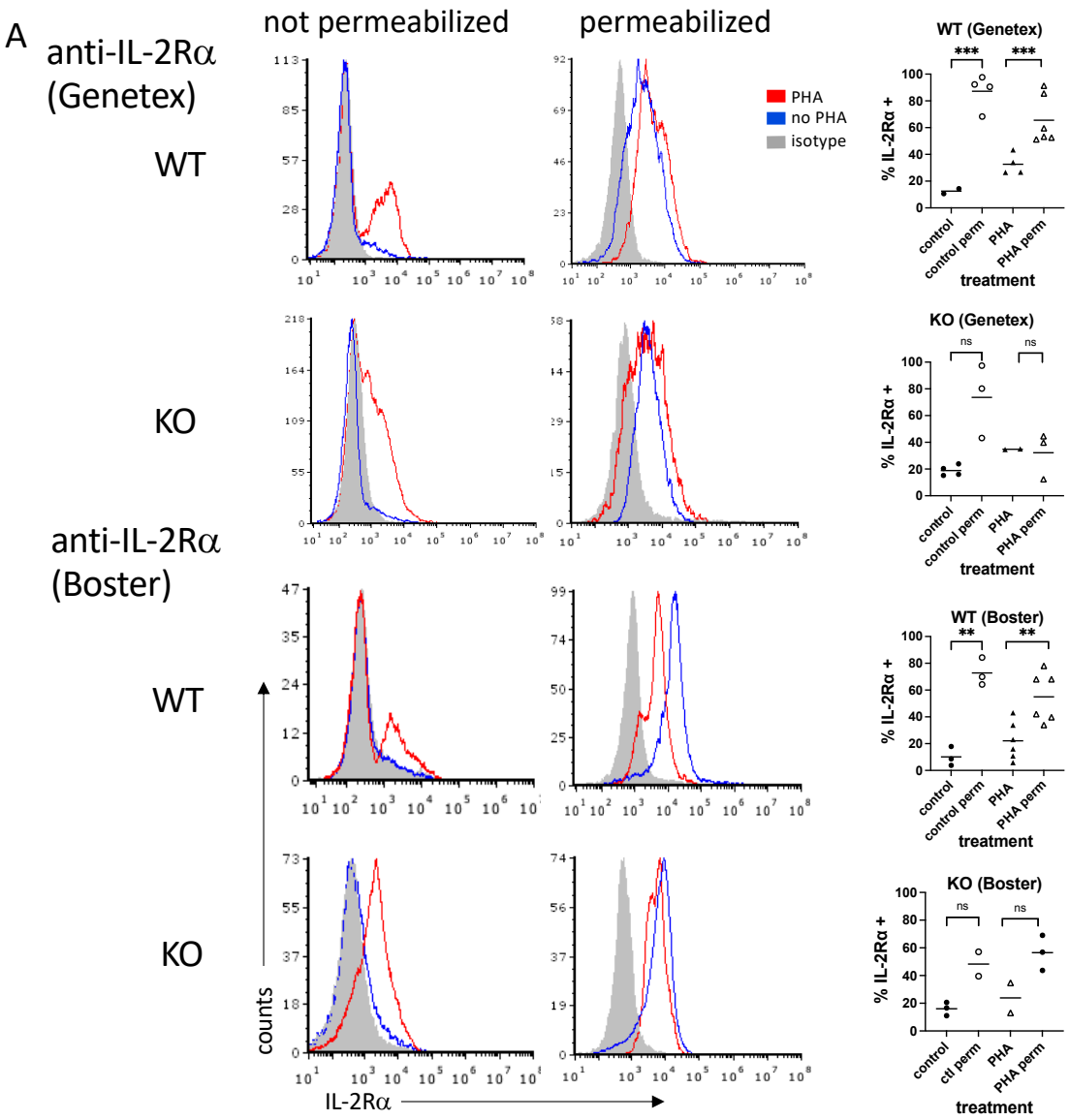
A
anti-IL-2Rα (Genetex)
WT
KO
anti-IL-2Rα (Boster)
WT
KO
not permeabilized
permeabilized
PHA
no PHA
isotype
counts
IL-2Rα
WT (Genetex)
KO (Genetex)
WT (Boster)
KO (Boster)
% IL-2Rα +
control
control perm
PHA
PHA perm
ctl perm
treatment
ns
***
**

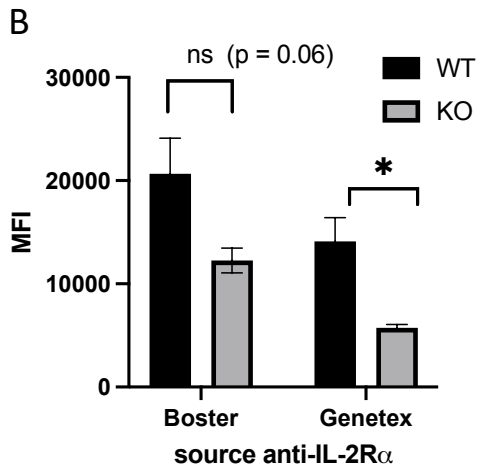
B
ns (p = 0.06)
*
WT
KO
MFI
30000
20000
10000
0
Boster
Genetex
source anti-IL-2Rα

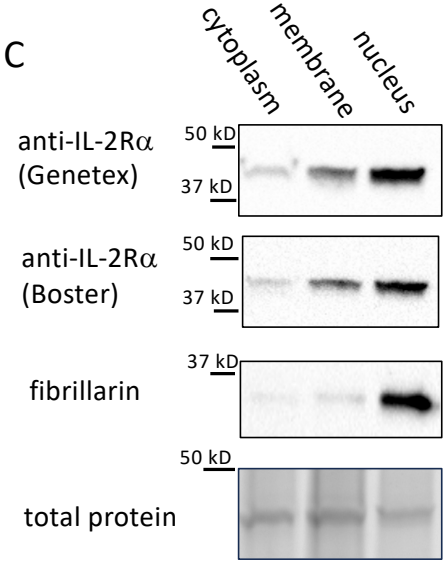
C
cytoplasm
membrane
nucleus
anti-IL-2Rα (Genetex)
anti-IL-2Rα (Boster)
fibrillarin
total protein
50 kD
37 kD

Figure 2

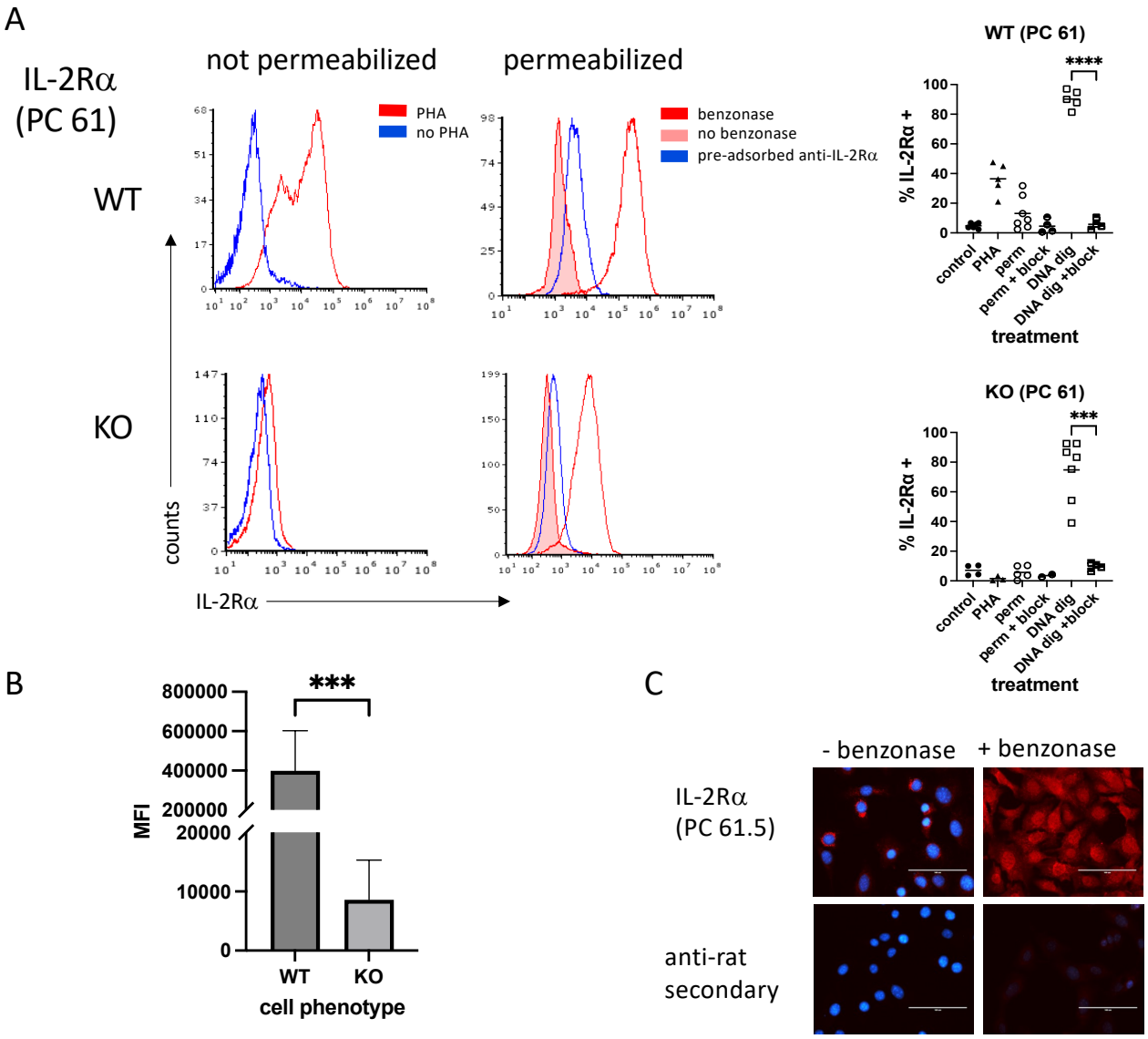
A
IL-2Rα
(PC 61)
not permeabilized
permeabilized
WT
KO
PHA
no PHA
benzonase
no benzonase
pre-adsorbed anti-IL-2Rα
counts
IL-2Rα
WT (PC 61)
KO (PC 61)
% IL-2Rα +
****
***
control
PHA
perm
perm + block
DNA dig
DNA dig +block
treatment
B
MFI
***
WT
KO
cell phenotype
C
- benzonase
+ benzonase
IL-2Rα
(PC 61.5)
anti-rat
secondary

Figure 3

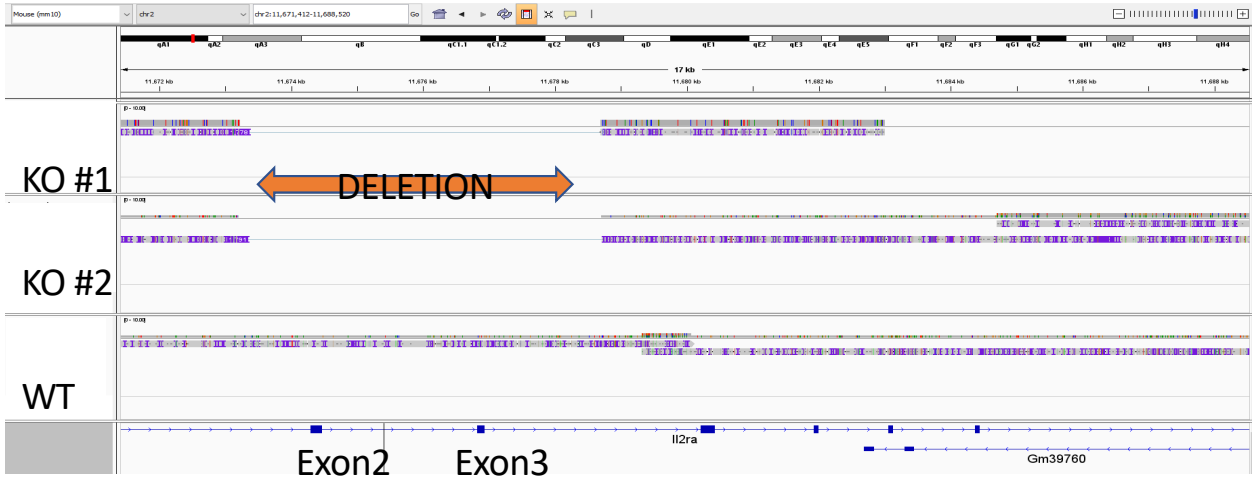


Figure 4

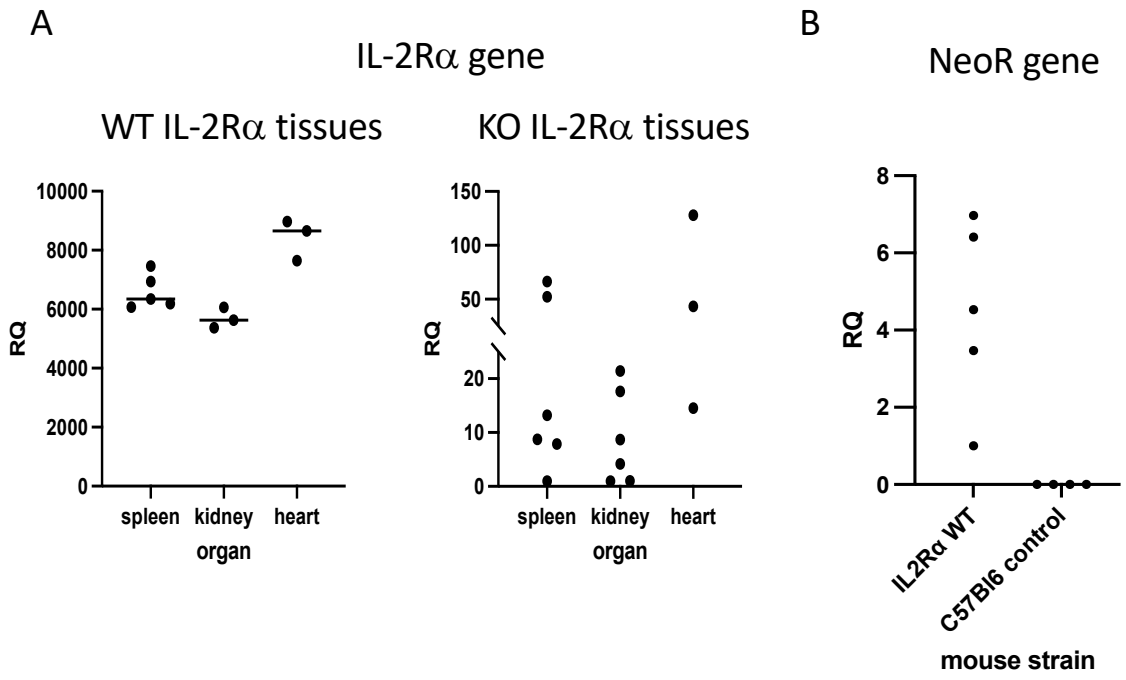
A
IL-2Rα gene
WT IL-2Rα tissues
KO IL-2Rα tissues
RQ
10000
8000
6000
4000
2000
0
spleen
kidney
heart
organ
150
100
50
20
10
0
B
NeoR gene
8
6
4
2
0
IL2Rα WT
C57Bl6 control
mouse strain

Figure 5

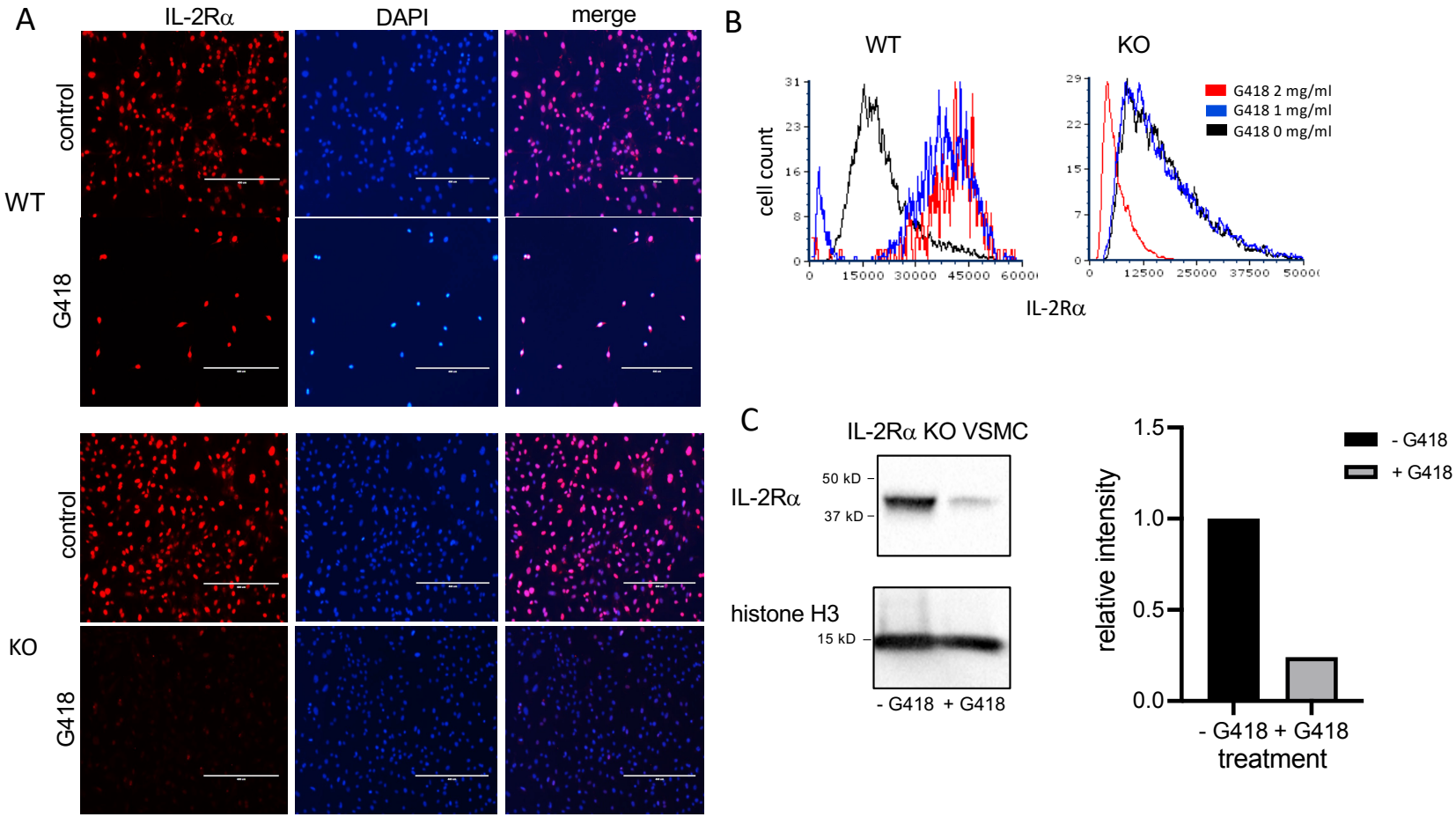
A
IL-2Rα
DAPI
merge
WT
control
G418
KO
control
G418
B
WT
KO
cell count
G418 2 mg/ml
G418 1 mg/ml
G418 0 mg/ml
IL-2Rα
C
IL-2Rα KO VSMC
IL-2Rα
50 kD
37 kD
histone H3
15 kD
- G418 + G418
relative intensity
- G418
+ G418
- G418 + G418
treatment

Figure 6

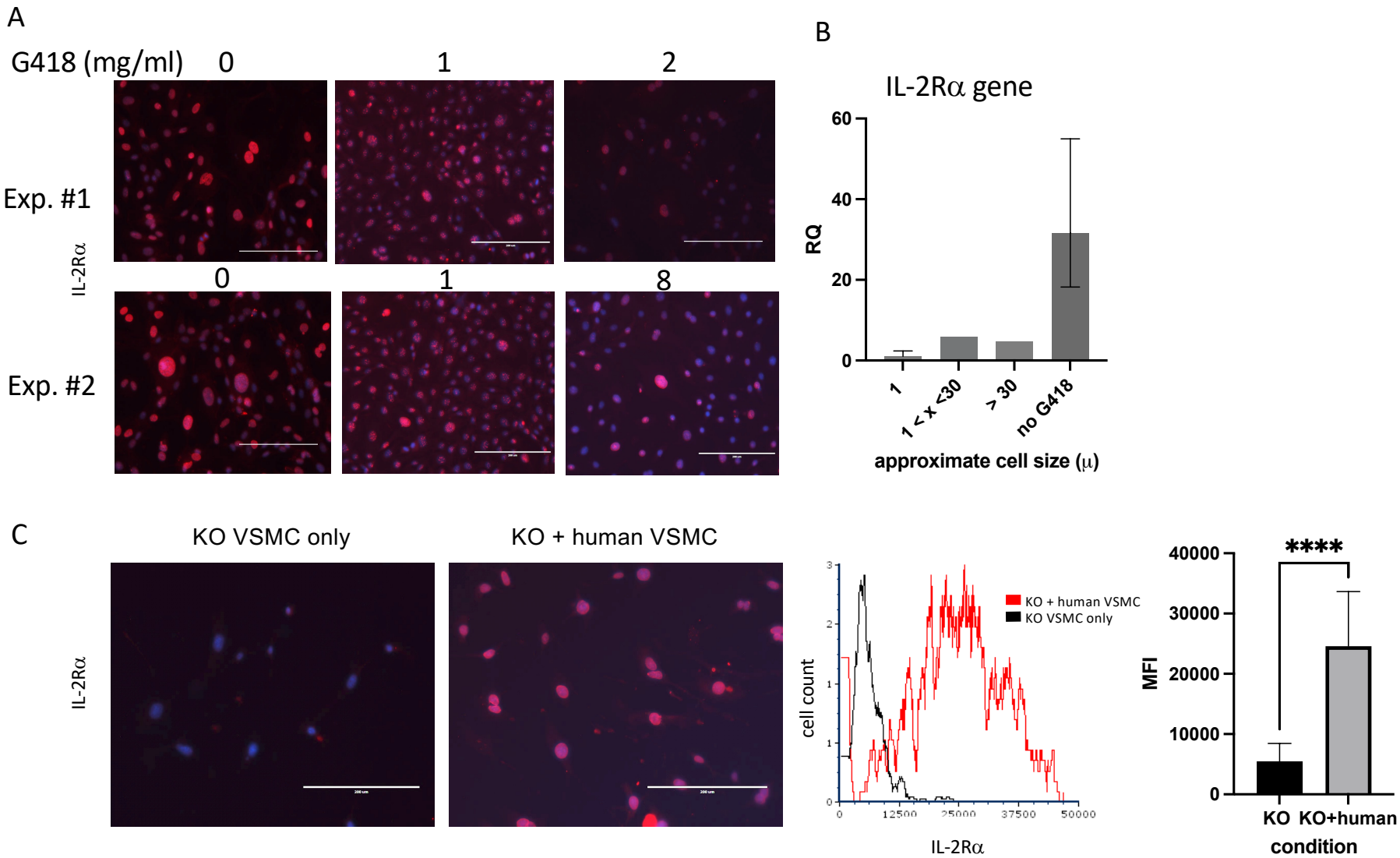
A
G418 (mg/ml)
0
1
2
Exp. #1
IL-2Rα
0
1
8
Exp. #2
B
IL-2Rα gene
RQ
60
40
20
0
1
1 < x <30
> 30
no G418
approximate cell size (μ)
C
KO VSMC only
KO + human VSMC
IL-2Rα
cell count
KO + human VSMC
KO VSMC only
0
12500
25000
37500
50000
IL-2Rα
MFI
40000
30000
20000
10000
0
****
KO
KO+human
condition

Figure 7

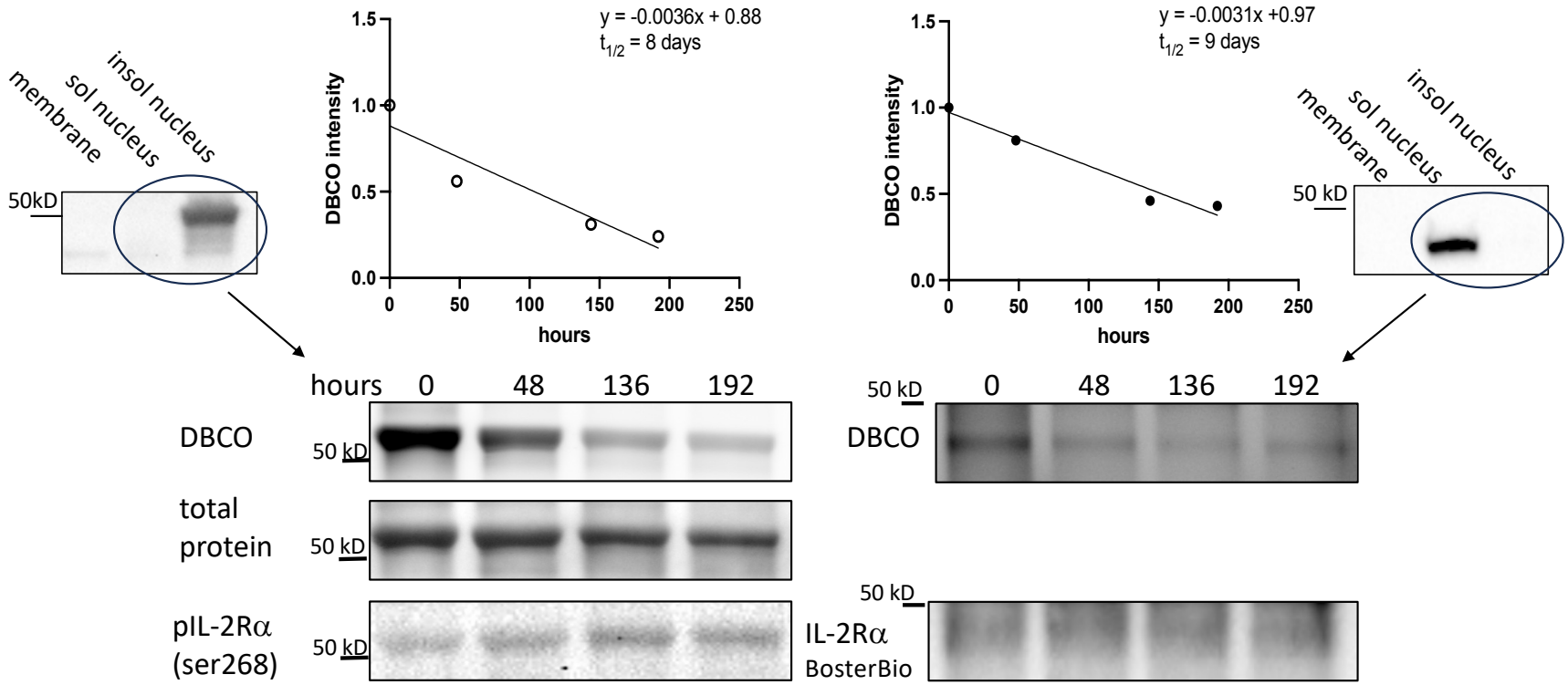
membrane
sol nucleus
insol nucleus
50kD
y = -0.0036x + 0.88
$t_{1/2}$ = 8 days
DBCO intensity
hours
y = -0.0031x +0.97
$t_{1/2}$ = 9 days
DBCO intensity
hours
membrane
sol nucleus
insol nucleus
50 kD
hours 0 48 136 192
DBCO
50 kD
total protein
50 kD
pIL-2Rα (ser268)
50 kD
50 kD
0 48 136 192
DBCO
50 kD
IL-2Rα BosterBio

Figure 8

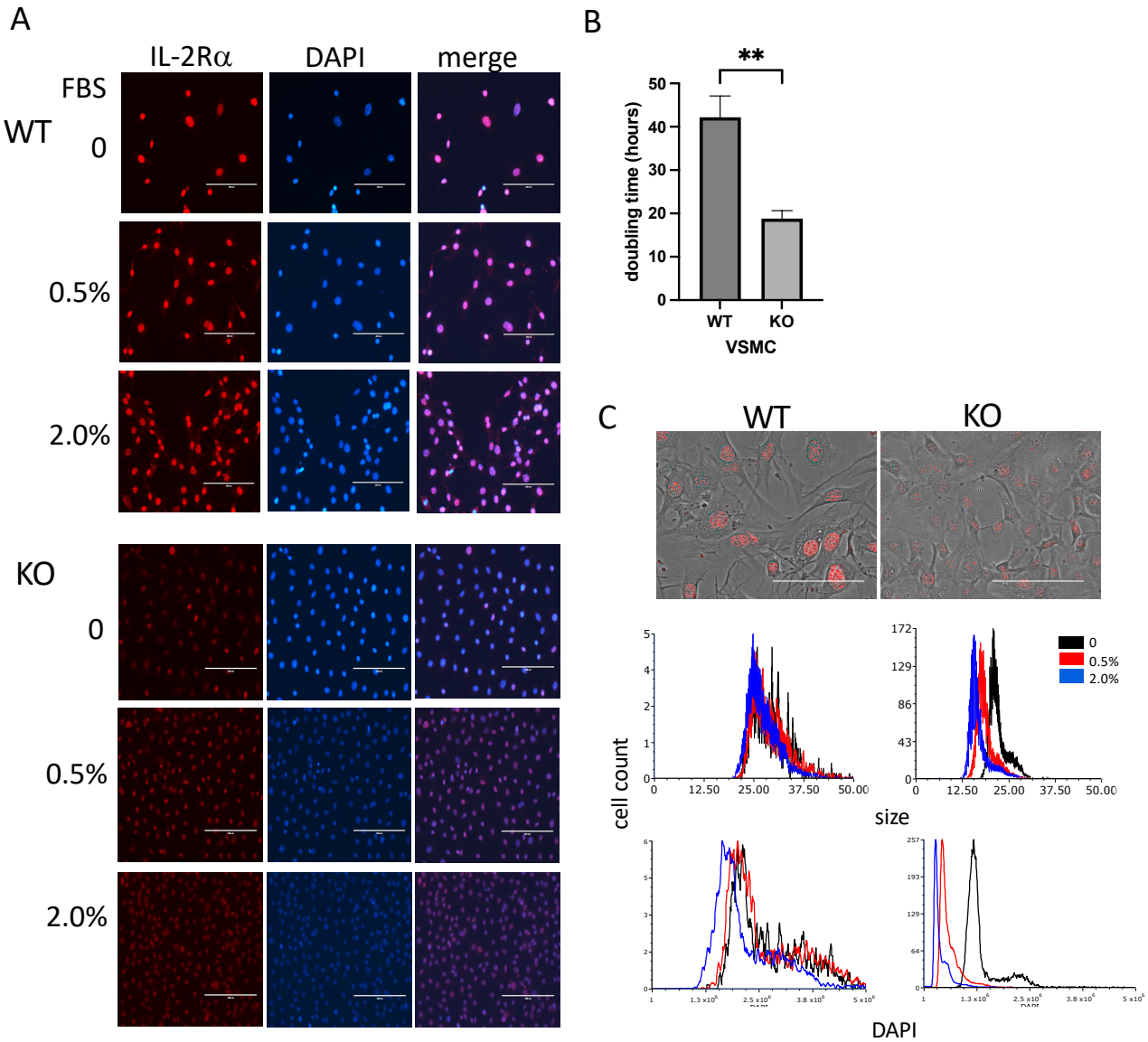
A
IL-2Rα
DAPI
merge
FBS
WT
0
0.5%
2.0%
KO
0
0.5%
2.0%
B
**
doubling time (hours)
50
40
30
20
10
0
WT
KO
VSMC
C
WT
KO
cell count
size
DAPI
0
0.5%
2.0%

Figure 9